

Field-Testing of Structure on Shallow Foundation to Evaluate Soil-Structure Interaction Effects

**Lisa M. Star,^{a)} M.EERI, Michael J. Givens,^{b)} M.EERI,
Robert L. Nigbor,^{c)} M.EERI, and Jonathan P. Stewart,^{c)} M.EERI**

A simple test structure was designed and constructed to facilitate forced-vibration testing of a shallow foundation experiencing combined base shear and moment demands. The structure consists of a reinforced concrete foundation and top slab separated by steel columns that can be configured with braces. The slabs have a 2:1 aspect ratio in plan view to facilitate variable amount of overturning for shaking in orthogonal directions. The structure was transported to two field sites with representative shear-wave velocities of approximately $V_S = 95$ m/s and 190 m/s. At each site, the foundation slab was cast-in-place. Forced vibration testing was conducted over a wide range of frequencies and load levels to enable the evaluation of foundation-soil stiffness and damping behavior for linear and nonlinear conditions. The data collected to facilitate such analyses include acceleration, displacement, and foundation pressure records (data can be accessed at DOI: 10.4231/D3NK3658M, DOI: 10.4231/D3HT2GC4G, DOI: 10.4231/D3D21RK0N). [DOI: 10.1193/052414EQS072]

INTRODUCTION

The importance of field-testing to measure soil-structure interaction (SSI) effects is associated with inherent limits of analytical models used to describe foundation stiffness and damping, which have generally been developed for idealized conditions such as rigid foundations and depth-invariant soil properties. Thus, testing is needed to evaluate model applicability for realistic field conditions and to guide the selection of input parameters. NIST (2012) summarizes existing models for predicting the stiffness and damping of foundation-soil interaction and current recommendations for adapting such models to field conditions.

Summaries of past SSI-related testing for the evaluation of foundation stiffness and damping can be found elsewhere (NIST 2012) and are not repeated here for brevity. However, we do wish to make a few key points to place the value of the present work in context:

^{a)} California State University, Long Beach, 1250 Bellflower Blvd, Long Beach, CA 90840

^{b)} Arup, 12777 West Jefferson Blvd Building D, Los Angeles, CA 90066

^{c)} University of California, Los Angeles, Civil & Environ. Eng. Dept., 5731 Boelter Hall, Los Angeles, CA 90095-1593

- First, while both field- and laboratory-scale tests can be used to measure foundation performance under dynamic loading, field-testing is preferred because radiation of energy away from the foundation into the surrounding soil medium is an important component of foundation-soil interaction, which cannot be adequately captured within the relatively small dimensions of laboratory models.
- Second, while field-testing can involve seismic loading (Tang et al. 1990, Wong and Luco 1990) or controlled forced vibrations (Lin and Jennings 1984, Crouse et al. 1990, Luco and Wong 1990, de Barros and Luco 1995, among others), forced vibration testing has some distinct advantages with respect to the evaluation of foundation stiffness and damping. One principal advantage relates to measurements of relative foundation/free-field motions, which comprise an essential test outcome (the desired quantities of foundation stiffness and damping are related to load/displacement ratios, and relative foundation/free-field motions comprise the denominator). In forced vibration testing, measured foundation motions are (allowing for noise effects) the desired differential motion, whereas in seismic loading the differential is difficult to establish because of spatial variations in ground motions.
- Third, while there are many cases of seismic loading having produced nonlinear SSI responses (Wong and Luco 1990, Stewart et al. 1999), previous forced vibration field tests of shallow foundations have not induced nonlinear soil responses causing substantial changes in soil properties relative to those for small strain (elastic) conditions.

In this paper, we describe a sequence of experiments in which the same structure is subjected to forced vibrations at multiple sites representing varying degrees of base flexibility. An essentially fixed-base condition is achieved in testing within a structural laboratory, whereas medium-stiff and soft soil conditions are present at the Garner Valley Downhole Array (GVDA) and Wildlife Liquefaction Array (WLA) field test sites, respectively. At both field tests sites, the structure was mounted on cast-in-place shallow mat foundations. Forced vibrations were applied on the top slab and foundation mat with two shaker systems that impart small and large force demands. Specimen responses were recorded with accelerometers, pressure cells, and displacement transducers. A data acquisition system was used with precise time stamping, which is important for interpretation of damping effects. The test structures were also instrumented to record earthquakes for several months between tests and following the completion of testing.

The full data set can be found online at <https://nees.org/warehouse/project/637>. Three test series are provided on NEEShub (2012a; Experiments 25 to 27) based on test location: (1) fixed-base testing, denoted as LAB; (2) WLA field-testing; and (3) GVDA field-testing. Each experiment included multiple trials with varying test conditions.

The value of the present test sequence is that it comprises field-testing (appropriate boundary conditions at multiple sites) over both a wide range of frequencies and loading amplitudes. As such, this data set affords the opportunity to evaluate the effects of nonlinearity on the frequency-dependent foundation responses, which has not been possible previously. In this data paper, we do not interpret the foundation responses, but instead describe the experimental set-up and instrumentation, and illustrate some useful aspects of the recorded data.

TEST STRUCTURE

The test superstructure consists of steel columns and braces supporting a concrete top slab, as shown in Figure 1. The steel members have the following attributes: (1) bolted connections to facilitate assembly in the field; (2) sufficient member capacity to prevent damage during testing, thus allowing re-use of the superstructure in multiple tests; (3) transportable from site-to-site; and (4) configurable bracing system to allow modification of superstructure stiffness. The top slab was designed to be nearly rigid against moment and shear deformations and to have sufficient mass that the soils underlying the foundation were likely to experience nonlinear responses during testing. The column-slab system has a high fixed-base natural frequency, between approximately 11 Hz and 35 Hz depending on the configuration and direction of shaking, to promote a strong effect of soil flexibility and damping on the system response.

The upper deck is composed of concrete with a nominal strength of 27.6 MPa reinforced with #7 grade 60 rebar and is 0.61 m thick, 4.28 m long and 2.13 m wide. The columns were constructed from four square hollow steel sections HSS 12'' \times 12'' \times 1/2'' (30.5 cm \times 30.5 cm \times 1.3 cm) that are 2.13 m tall and have a mass of approximately 250 kg each. The removable cross-braces are constructed from HSS 4'' \times 4'' \times 1/2''

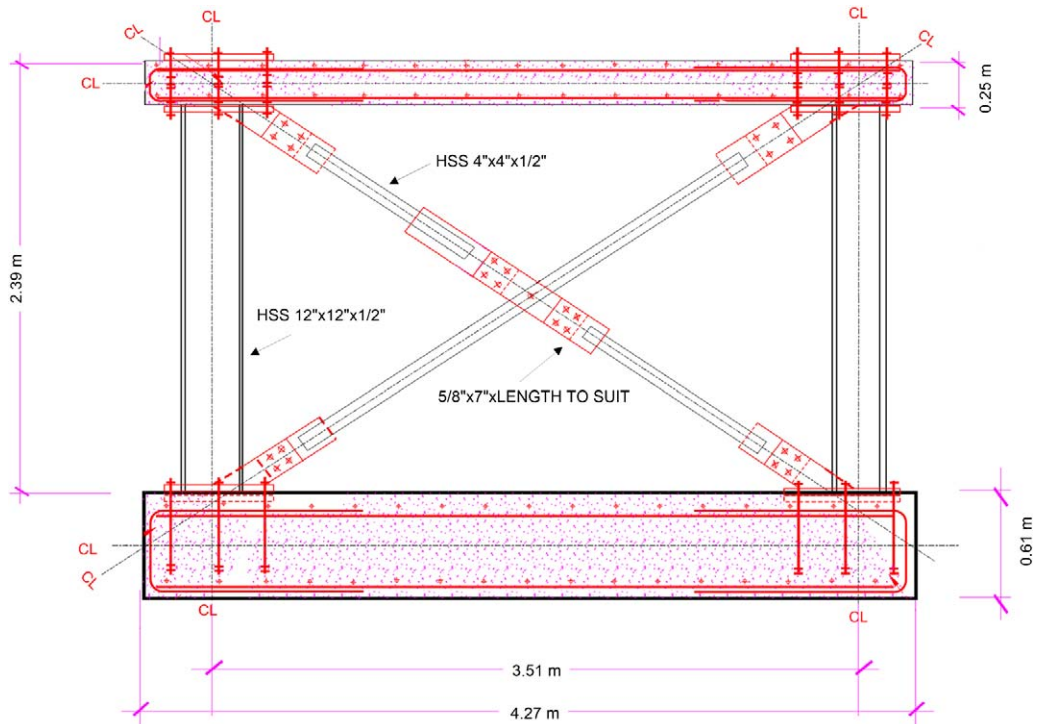


Figure 1. Configuration of the UCLA portable SSI test structure.

(10.2 cm × 10.2 cm × 1.3 cm) steel sections. The total mass of the braces is approximately 800 kg.

The foundations of the test structure consisted of simple mats constructed at grade and poured in place to ensure realistic foundation-soil contact. The foundation of the test structure is sufficiently thick to be nearly rigid, so as to avoid damage during the large-amplitude tests and to ensure compatibility with SSI analytical models. The foundation mat is composed of concrete with a nominal strength of 27.6 MPa concrete reinforced with #5 grade 60 rebar. The concrete foundations had more than 28 days to cure before testing. Based on the dimensions and unit weight, the foundation has an estimated mass of 13,340 kg. Nine 2.54 cm diameter threaded rods were used to anchor the base plate of each column of the super structure to the foundation. The anchors were pre-drilled and secured using epoxy. The super structure and foundation together are 3 m tall.

TEST SITES

STRUCTURAL LAB

The UCLA Structural Engineering Laboratory (LAB) is fitted with a 1.5 m thick reinforced concrete strong floor. As shown in Figure 2, DYWIDAG threaded bars are embedded in the strong floor on a 0.6 m grid and allow the test structure to be tied directly to the floor, leading to an effectively fixed-base condition.

WILDLIFE LIQUEFACTION ARRAY (WLA) TEST SITE

The Wildlife Liquefaction Array (WLA) is maintained by NEES@UCSB ([NEEShub 2012b](https://nees.ucsb.edu); nees.ucsb.edu/facilities/wla). Figure 3 shows a plan view of the site. WLA is located



Figure 2. Test structure connection to the LAB site strong floor.

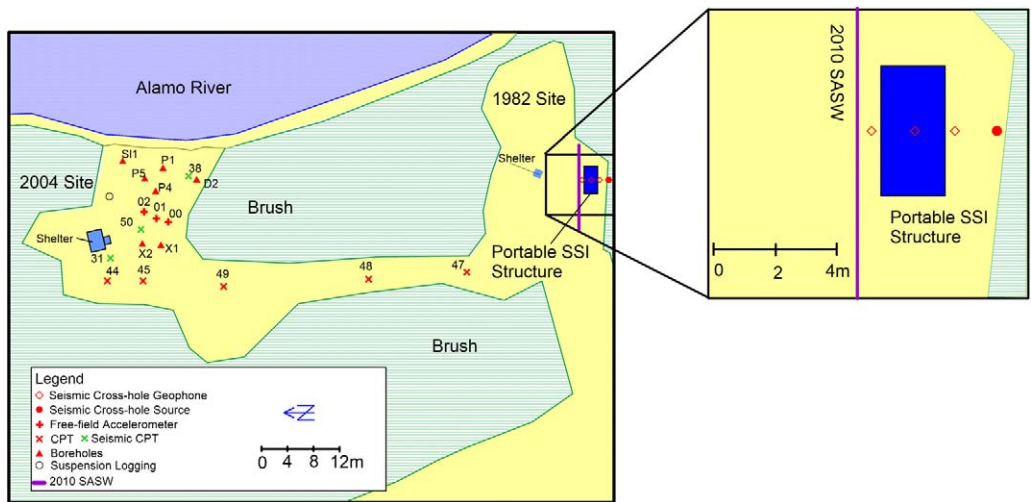


Figure 3. Plan view sketch of the WLA site showing locations of the various geophysical site characterization tests.

on the west bank of the Alamo River, 13 km north of Brawley, California. WLA was instrumented with a vertical array in 1982 to study liquefaction (Youd and Holzer 1994). Several significant earthquakes have been recorded at this site, including the first direct measurement of dynamic pore pressure during liquefaction in 1987 (Youd et al. 2004a). The site was expanded and updated in 2004 as a NEES field test site (Steidl et al. 2004). Figure 3 shows two general instrument locations marked as the “1982 site” and “2004 site.”

Geotechnical investigations at the WLA site include borings with standard penetration testing, cone penetration test (CPT) soundings, and laboratory testing of soil samples (Youd et al. 2004b). As shown in Figure 4, field tests indicate laterally consistent soil conditions, with 2.0–3.0 m of silty clay to clayey silt overlying silt, silty sand, and sandy silt that is 3.0–4.0 m thick. This relatively coarse layer is underlain by silty clay to clayey material. The average moist unit weight of the soil is approximately 17.0 kN/m^3 . The water table depth varies seasonally from 1–2 m below the ground surface. These measurements are from the 2004 site portion of WLA.

Geophysical data for the site has been developed from seismic CPT downhole measurements, suspension PS logging (Youd et al. 2004b), and Spectral-Analysis-of-Surface-Waves (SASW) measurements (Stokoe et al. 2010) conducted at the time the NEES@UCSB site was established and supplemental measurements made near the location of the SSI test structure. As shown in Figure 3, the locations of prior measurements are principally at the 2004 site portion of WLA, which is approximately 70 m from the “1982 site” adjacent to the SSI test structure. As part of the present work, SASW testing was performed adjacent to the test structure (Stoke et al. 2010). Seismic crosshole testing was also performed across the structure’s footprint before and after specimen construction. The SASW and crosshole testing locations are shown in Figure 3. The crosshole survey was conducted in three phases to

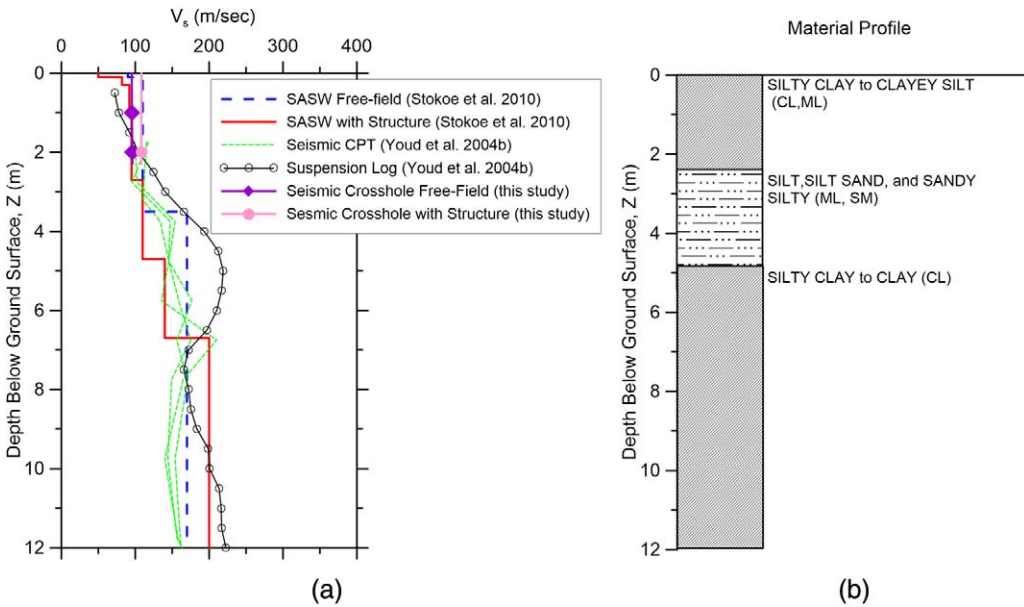


Figure 4. Subsurface characteristics based on site exploration of the WLA site: (a) free-field shear wave velocity profile and (b) material profile.

evaluate the influence of the structural weight on seismic velocities. Initial crosshole testing was performed on 17 November 2009, before construction, 20 November 2009, following construction of the foundation and on 17 December 2009, and 25 May 2011, following installation of the full structure. The crosshole testing was performed at depths of 1 m and 2 m. As shown in Figure 4, the crosshole testing indicates seismic velocities in the upper 1–2 m of about $V_S = 95$ m/s prior to construction and 108 m/s following construction.

GARNER VALLEY DOWNHOLE ARRAY (GVDA) TEST SITE

The Garner Valley Downhole Array (GVDA) site is also maintained by NEES@UCSB (NEEShub 2012b; nees.ucsb.edu/facilities/gvda). Figure 5 shows a plan view of the site. As shown in Figure 6, the GVDA site includes a permanent steel moment frame structure with a reinforced concrete roof and foundation, referred to here as the UCSB permanently installed SSI structure. Details on the dimensions and mass of this structure are provided in Tileyliglu et al. (2011) and at the NEES@UCSB website. The permanent structure is situated approximately 4.6 m to the south of the portable structure considered in the present work. During this series of tests the permanent structure was unbraced.

Geotechnical investigations at the GVDA site include borings with standard penetration testing, cone penetration test (CPT) soundings, and laboratory testing of soil samples (Youd et al. 2004b). As shown in Figure 7, the site profile consists of 18–25 m of lake-bed alluvium consisting principally of silts and clays near the ground surface transitioning to relative coarse sands and silty sands below approximately 6 m. Underlying the alluvium is decomposed

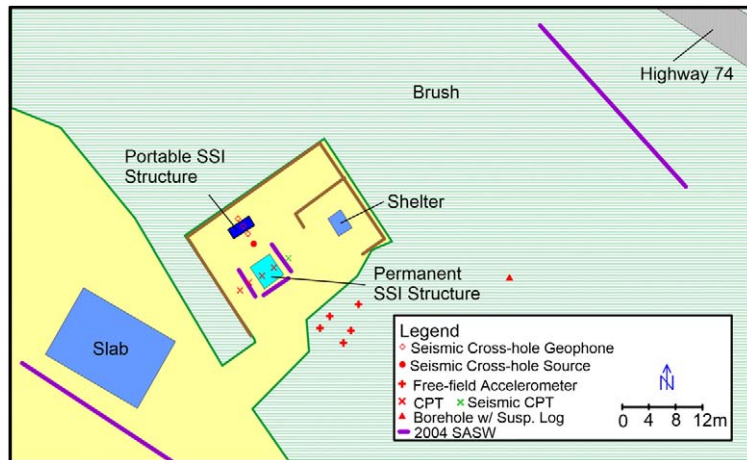


Figure 5. Plan view of the GVDA site showing the approximate locations of geophysical tests.



Figure 6. Photograph showing the portable test structure (right) and the previously constructed permanent structure (left) located at GVDA

granite, which extends to depths of about 91 m, where competent granodiorite bedrock is encountered. The average moist unit weight of the soil varies from 17.3 kN/m^3 to 19.6 kN/m^3 . The water table ranges seasonally from 0 m to 3 m below the ground surface. As shown in Figure 7, geophysical data from the site is available from [Stokoe et al. \(2004; SASW\)](#), [Youd et al. \(2004b; downhole\)](#), and [Steller \(1996; suspension logging\)](#).

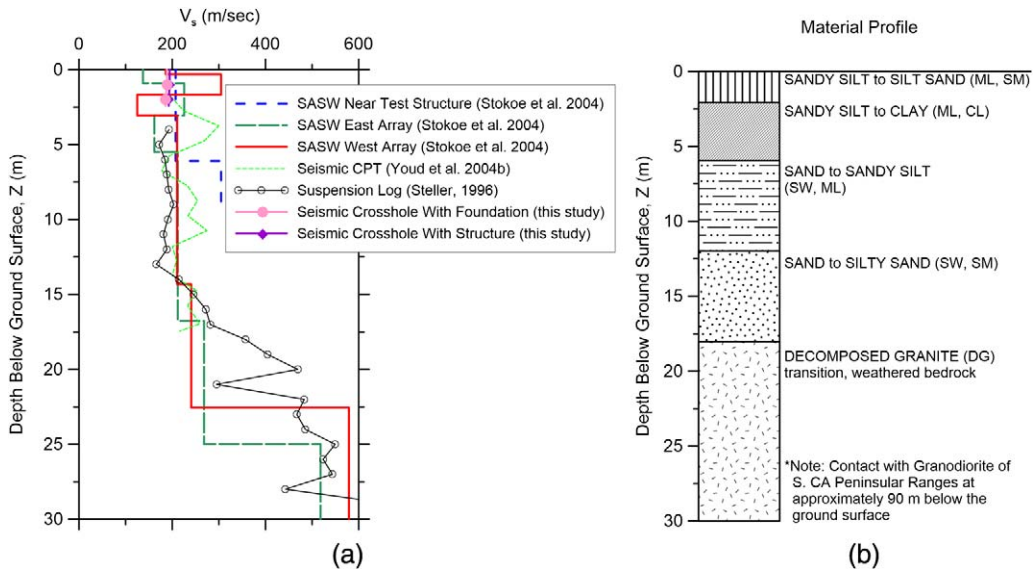


Figure 7. Subsurface characteristics based on site exploration of the GVDA site: (a) shear wave velocity profile and (b) material profile.

As part of the present work, a crosshole seismic survey was undertaken on 26 May 2011 to evaluate V_s within the upper two meters of the soil column below the structural footprint. A direct measurement of the V_s of the soil was not performed prior to construction of the concrete slab foundation. In an effort to back-calculate the V_s with no influence from the structural weight the survey was performed in two phases. Cross-hole testing was initially performed across the structural footprint with only the weight of the foundation, followed by testing after the installation of the full structure. As shown in Figure 7, the cross-hole testing indicates seismic velocities in the upper 1–2 m of about $V_s = 187$ m/s with the foundation in place and 194 m/s following the complete structure installation. Based on these results, the scaling of V_s with overburden pressure was evaluated using (adapted from Tileylioglu et al. 2011):

$$\frac{(V_s)_1}{(V_s)_2} = \left(\frac{\sigma'_{v0} + (\Delta\sigma_v)_1}{\sigma'_{v0} + (\Delta\sigma_v)_2} \right)^{n/2} \quad (1)$$

where $(V_s)_1$ and $(V_s)_2$ are the overburden-consistent shear wave velocities for a particular depth z , σ'_{v0} is the effective stress from the soil's self-weight at depth z , and $(\Delta\sigma_v)_1$ and $(\Delta\sigma_v)_2$ are the increment of vertical stress at depth z from varying structural weights (e.g., for combined foundation/structure and foundation alone, respectively). The $\Delta\sigma_v$ quantities were computed using classical "Boussinesq-type" stress distribution theory (e.g., Fadum 1948). The n value typically varies from approximately 0.5 for granular soils to 1.0 for cohesive soils with plasticity index $PI > 6.5$ (Yamada et al. 2008). A site-specific n value of 0.6 was back-calculated for a depth of 1.5 m below ground surface from Equation

using the aforementioned cross-hole velocities at a depth where $\sigma_{v0}' = 25 \text{ kN/m}^2$, $(\Delta\sigma_v)_1 = 10 \text{ kN/m}^2$ and $(\Delta\sigma_v)_2 = 6.3 \text{ kN/m}^2$.

The velocity that is expected at the site prior to foundation placement was then derived in a similar manner to Equation 1:

$$V_S \approx V_{S0} \left(\frac{\sigma_{v0}' + \Delta\sigma_v}{\sigma_{v0}'} \right)^{n/2} \quad (2)$$

where V_{S0} denotes the pre-construction, free-field shear wave velocity. Based on Equation 2 we find $V_{S0} = 176 \text{ m/s}$ for a depth of 1.5 m using the site-specific $n = 0.6$, $V_S = 194 \text{ m/s}$, $\sigma_{v0}' = 25 \text{ kN/m}^2$ and $\Delta\sigma_v = 10 \text{ kN/m}^2$.

INSTRUMENTATION AND SHAKERS

SENSORS

Figure 8 shows the orientations of the coordinate axes relative to the foundations and the locations of sensors for the GVDA test. Similar diagrams are given in Appendix Figures A1 and A2 for LAB and WLA, respectively. Vibration modes for translation are represented by x , y , and z , while rotation about these axes, respectively, are xx , yy , and zz . The portable structure was instrumented with eight Kinometrics EpiSensor ES-T triaxial accelerometers. The accelerometers have a selected output range of $\pm 20 \text{ V}$, for an amplitude range of $\pm 4.0 \text{ g}$. The bandwidth is DC to 200 Hz. Accelerometers have calibrated sensitivities of $5.00 \pm 0.02 \text{ volts per g}$. One triaxial accelerometer was bolted in place at each corner of the structure top slab and foundation slab. At the GVDA test site, the permanent structure was instrumented with four triaxial accelerometers, three on the base slab, and one on the roof. At the soil sites, additional triaxial accelerometers were installed in the soil between 1.5–4.3 m from the structure in both the positive x and the positive y -directions. Both were located at the elevation of the foundation base.

Artificial phase delays are introduced into digital data from sensors, data acquisition equipment, and data processing. This is particularly a concern when different sensors and data acquisition systems are used. Unaccounted for, these phase delays could introduce errors in the evaluation of structural response characteristics, especially the complex damping behavior that is part of SSI. A well-designed instrumentation system will have a phase response that is a linear function of frequency. This results in a constant group delay, defined as the derivative of phase delay with frequency. The Kinometrics ES-T accelerometers are designed to have a linear phase response from 0 radians at 0 Hz to about 2 radians at 200 Hz (1,257 rad/sec), giving a constant group delay of about 0.0016 rad-sec. Constant group delay will result in the time delay of the amplitude envelope at various frequencies being equal across the frequency range, preserving the time domain wave shape. Further, the Kinometrics ES-T accelerometers are very closely matched, within 1% for phase and 0.2% for amplitude (Kinometrics 2005).

During loading with the eccentric mass shaker at the two soil sites, two data acquisition systems were required: one for the principal set of instrumentation used in the tests and a second related to the shakers themselves. To facilitate synchronization of these two data streams, we installed sets of accelerometers side-by-side, with one set each on the shaker

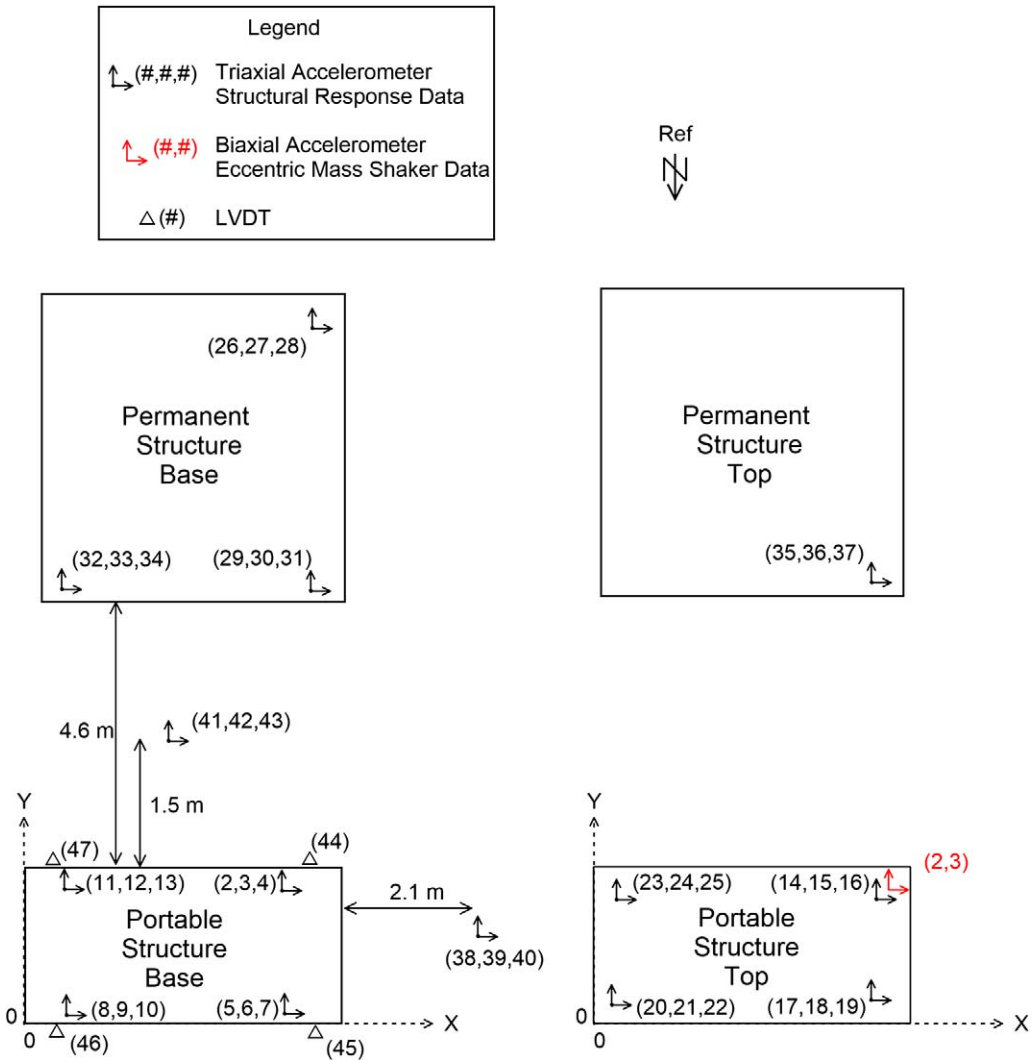


Figure 8. Sketch showing the structures and sensors for the 2009–2011 GVDA tests.

and main data-acquisition systems. As shown in Figure 8, these are channels 15 and 16 (main system) and 2 and 3 (shaker system). Figure 8 and Appendix Figure A.1 show the locations of these two accelerometers in red.

Four Trans-Tek, Inc., model 0244-0000 DC LVDTs (linear variable differential transformers) were installed near the corners of the foundation mat during high amplitude loading to measure the relative displacement between the foundation and surrounding soil. The LVDTs have a measurement range of up to 5 cm and frequencies ≤ 300 Hz.

Eight custom pressure cells were installed under the foundation at the WLA site. Each cell is approximately 10 cm in diameter and 3 cm high. The pressure cells were arranged in

two concentric rectangles in order to measure pressure at the interior and exterior of the foundation slab. The interior pressure cells have a maximum capacity of 137 kPa and the exterior cells have a maximum capacity of 274 kPa.

The permanently installed WLA instrumentation maintained by NEES@UCSB was used to record ground motions from earthquake loading. The sensors used in this study are shown as 00, 01, and 02 in Figure 3 and discussed at nees.org/warehouse/experiments/353. They are assumed to represent free-field conditions.

Further details about the EpiSensor accelerometers and LVDTs can be found at the NEES@UCLA website (nees.ucla.edu/equipment.html). More details about the pressure sensors can be found in Star (2011).

VIBRATION SOURCES

The test structure was subjected to forced vibration testing using two types of shakers, one a linear shaker that provides small-amplitude force demands and a second eccentric mass shaker that provides larger-amplitude force demands. Additional vibration at the sites was provided using a large Tri-Axial Vibroseis vehicle and naturally occurring earthquakes. Forced vibration testing was performed between September 2009, and August 2011.

The linear mass shaker was a small portable Acoustic Power System “ELECTROSEIS” model 400 long stroke shaker. The shaker mass is 7.3 kg and it can induce a maximum force of 440 N. The shaker was controlled by an APS Dynamic Inc. dual mode power amplifier model 144 and a HP Agilent 33220A, 2 MHz function / arbitrary waveform generator. Waveforms applied to the specimen included continuous linear frequency sweeps and step frequency sweeps. Linear sweep loading consisted of nearly constant amplitude force with variable frequencies ranging from 4–54 Hz. Frequency step loading also had nearly constant-amplitude force and constant frequency loading within short intervals. Frequencies were increased in 0.5 Hz steps over the same frequency range as the sweep loading. The linear mass shaker was used for *x*- and *y*-direction and torsional (*zz*) forced vibration testing at the roof and at the foundation level.

The eccentric mass shaker was a large AFB Engineered Test Systems Model 4600A maintained and operated by NEES@UCLA. The eccentricity of the circular weights was adjusted from 0 N-m to 110 N-m and had an operating loading frequency range of 0–20 Hz. The shaker force was computed as:

$$F = m_r r \omega^2 \cos \alpha + (m_r + m_b) \ddot{u} \quad (3)$$

where m_r is the rotating mass, m_b is the non-rotating mass portion of the shaker, r is the radius from the center of rotation to the centroid of the rotating mass, ω is the angular frequency, α is the angular position of the rotating mass, and \ddot{u} is the translational acceleration of the shaker base (after Reinert et al. 2012). The first portion of Equation 3 represents shaker force due to rotation of the eccentric mass and the second component is shaker force due to translation of the shaker mass center. Forcing frequencies were controlled by a custom National Instruments–based controller. For consistency with the forced vibration testing performed with the linear mass shaker, continuous sweeps and frequency steps were performed. Continuous sweep loading frequencies ranged from 0–19 Hz. Step loading was applied using

0.2 Hz steps spanning the same 0–19 Hz frequency range. The eccentric mass shaker was used for x - and y -direction forced vibration testing at the roof level.

Loading was also provided by a large triaxial Vibroseis vehicle that has a peak force of 267 kN in the vertical direction and 134 kN in the horizontal directions. The peak force can be reached over a frequency range from 12–180 Hz in the vertical direction and 5–180 Hz in the horizontal directions. The Vibroseis vehicle is maintained and operated by NEES@UTexas. It was located approximately 20 m from the test structure and was used to shake the ground at the WLA test site. Vibrations as large as about 0.15 g were measured in the soil near the test structure.

Details about the linear and eccentric mass shakers can be found at nees.ucla.edu/equipment.html. More details about the Vibroseis vehicle are available at nees.utexas.edu/Equipment.shtml.

Earthquake shaking was also recorded on the test structure while it was at the WLA site. Table 1 summarizes the attributes of earthquakes recorded. Using information available on the USGS website (earthquake.usgs.gov), we identified the earthquake magnitudes and hypocenter locations near the California/ Mexico border, approximately 50 km south of the WLA test location. These are likely aftershocks of the 4 April 2010 M 7.2 El Mayor Cucapah earthquake.

DATA ACQUISITION

The principal data collection function was performed by eight Kinometrics Quanterra Q330 wireless data loggers. The Q330s have six analog input channels, global positioning system (GPS) receivers for precision timing, and 24-bit digital resolution. Absolute timing accuracy is <10 microsecond, and the sample clocks are slaved to GPS. The Q330 data were collected on a PC hard drive using Kinometrics' Rockhound data acquisition software. The sampling rate was 200 samples per second per channel. The Q330 digitizer uses a sigma-delta A/D converter with multiple stages of low-pass filtering and decimating that introduces a time delay. There is no channel-to-channel skew because there is a separate A/D converter for each channel. We sampled at 200 Hz with a final anti-alias filter at 80 Hz and a linear-phase finite impulse response (FIR) filter for all measurements, which produces a combined constant group delay of 0.09 sec in conjunction with the previously mentioned accelerometer constant group delay. Therefore, as a result of using identical, high precision sensors and

Table 1. Earthquake loading recorded at WLA

Date	Local Time	Epicenter Location	Magnitude (M)	Epicentral Distance (km)	Depth (km)
8 May 2010	11:31:17 AM	32.728°N 115.835°W	3.4	49.9	10.9
8 May 2010	11:33:11 AM	32.675°N 115.806°W	5.0	53.5	6.0
8 May 2010	11:35:12 AM	32.669°N 115.827°W	3.0	55.1	1.3
8 May 2010	11:41 AM	?	2.4	?	?
8 May 2010	11:46:27 AM	32.675°N 115.811°W	4.9	53.8	14.0
8 May 2010	11:46 AM	?	?	?	?

identically matched data acquisition (DAQ) channels, the presence of the delay is not evident in the data files.

Data acquisition channels for each experiment and trial are described in Tables A1–A3 in the electronic supplement. Data from this acquisition system is referred to as “structural response data.”

During forced vibration testing using the eccentric mass shaker at the two soil sites, pulse data, which marks in time the beginning of each mass rotation cycle, and accelerometer data from two high-frequency uniaxial horizontal accelerometers, were recorded using a separate National Instruments DAQ system which had a sampling rate of 5,000 Hz. The higher sampling rate is necessary in order to determine phasing of the shaker force with adequate precision. The data acquisition channels used for testing with the eccentric mass shaker are given in Tables A1–A3. In this paper, the data from this acquisition system is referred to as “eccentric mass shaker data.” The correlation method used to match the eccentric mass shaker data and the structural response data is described in the “Synchronized Structural Response and Eccentric Mass Shaker Data Files” section below.

In addition to these two data acquisition systems, the permanently installed WLA data acquisition system maintained by NEES@UCSB was used to record ground motions from earthquake loading. More information about the data acquisition system can be found at the NEES@UCSB website. The data from this system is referred to as “free-field earthquake data.”

TRIALS AND DOCUMENTATION

The test series at LAB, WLA, and GVDA are documented as Experiment Nos. 25 through 27, respectively. Each experiment consisted of several trials. The loading and structural conditions for each trial are summarized in Table 2. Each trial consisted of multiple repetitions of loading in multiple directions (x , y , and torsion). Unprocessed data, converted data, and corrected data files, were created for each trial repetition, as discussed below.

Tables A4 through A6 show field-testing logs for the forced vibration testing performed at LAB from 17–21 September 2009, at WLA 17 December 2009 to 25 May 2010, and at GVDA from 22 June to 2 August 2011.

The highlighted blue rows in Tables A4–A6 represent the unprocessed data files, which contain several different forced vibration testing runs. The underlying non-highlighted rows represent the subevents with descriptions of the SSI system, the loading, load frequency and time length provided. Each subevent was assigned an identification string based on the test location, trial number, subevent number, and repetition. The first number in the string refers to the test location. The three test locations have been given the following numbering: 1 = LAB, 2 = WLA and 3 = GVDA. At the GVDA test location, the second number in the string refers to the trial number, at WLA it refers to the trial number minus one (so trial 3 is listed as 2), and at the LAB location all trials are given the number 0. The third number in the string is the subevent order number, which was based on the chronology of testing within a particular trial. If the subevent number has a letter following the order number, this letter represents the order of repetition of a common type of vibration force, duration and frequency range. For example, in Table A5a Exp.2.0.1b represents

Table 2. Experiments and trials

Experiment	Trial	Loading type	Structure configuration
25	1	EMS	Braced
	2	Hammer, EMS	Unbraced
	3	Hammer	Braced
26	1	LMS	Braced
	2	LMS	Braced, unbraced
	3	EMS	Braced, unbraced
	4	VSV	Unbraced
	5	Earthquake	Unbraced
27	1	LMS	Braced
	2	EMS	Braced
	3	LMS	Unbraced
	4	EMS	Unbraced

Notes: LMS: Linear Mass Shaker; EMS: Eccentric Mass Shaker; VSV: Vibroseis shaker vehicle; Hammer: hammer impact; Unbraced: unbraced structure; Braced: braced structure.

experiment at WLA, trial 1, first forced vibration test of the trial, and “b” represents redundancy with this test being the second of its type.

Two data acquisition systems were used for WLA Trial 3 (eccentric mass shaker). Table A5c provides logs for the structural response data and the corresponding eccentric mass shaker data. Similarly, for GVDA Trials 2 and 4 (eccentric mass shaker) Tables A6b and A6d provide logs for the structural response data and the corresponding eccentric mass shaker data.

DATA PROCESSING

Data collected during the experiments can be grouped into three main categories: structural response (SR) data for all trials, eccentric mass shaker (EMS) data, and data from permanently installed field instrumentation for earthquake loading trials. Each data set required different processing, which is described here.

UNPROCESSED DATA FILES

Three types of unprocessed data are available: structural response data, eccentric mass shaker data, and free-field data files from earthquake loading events.

Unprocessed Structural Response Data Files

The unprocessed structural response data is stamped in Unix time and all other channels are recorded in machine counts. Unix time is a system describing time as a real number in decimal seconds from 1 January 1970 in the Greenwich Mean Time (GMT) zone. The testing was performed in California, which is within the Pacific Standard Time (PST) zone, eight hours behind GMT. Testing between March and November used Pacific Daylight Time (PDT), which is seven hours behind GMT.

The unprocessed data is labeled according to the date and GMT (YYYYMMDDGMT) when the recording began. For example, a test recorded with a beginning PDT of 11:40 a.m. and 43 seconds on 20 May 2010 would have a text filename of 20100520184043.txt. The structural response unprocessed data files are listed in Tables A4–A6. The recorded data channels are given in Tables A1–A3 for each trial.

Unprocessed Eccentric Mass Shaker Data Files

The unprocessed eccentric mass shaker data is recorded with respect to relative time in seconds from beginning of file recording. All other channels are recorded in digital counts. At WLA the unprocessed eccentric mass shaker data is labeled based on designated trial numbers as shown in Table A5c. At GVDA the unprocessed eccentric mass shaker data is labeled according to the date and PST/PDT (GV_YY_MM_DD_PST/PDT) when the recording began, as shown in Tables A6b and A6d).

Unprocessed Free-Field Earthquake Data Files

During earthquake loading, free-field data files were collected from data archived from the permanently installed field accelerometers from the NEES@UCSB Wildlife Liquefaction Array. Acceleration records from these sensors were not collected following forced vibration tests. Figure 1 indicates the locations of field instrumentation from which data was collected. The unprocessed free-field earthquake data files were obtained for WLA Trial 5 (earthquake loading). The data files contain a single directional accelerometer response with a GMT time signature. The acceleration is in engineering units (cm/sec^2). The files are labeled based on a site code for WLA, description symbols, location identification number, date and recording start time. For example, file “5210.HNE_00.2010.127.01.30” can be interpreted for our project starting at the last letter, with “E” meaning east direction, 00 is the sensor identification number (see Figure 1), 2010 is the year, 127 is the 127 day of the year at 1:30 GMT. The three directional of the accelerometers used are N (north), E (east), and Z (vertical).

CONVERTED DATA FILES

Converted data was produced by dividing the unprocessed data into individual subevents and converting data into engineering units. Raw digital counts were converted to volts by dividing integer counts by 41,9430 ($2^{24}/40$) counts per volt. Acceleration signals in volts were converted to “g” using a sensitivity of 5.00 volts per g. The LVDT and pressure cell records were converted to engineering units (in. and kPa respectively) using individual instrument calibrations in conjunction with the battery source voltage. The conversion units used are provided in Tables A2–A3. Converted structural response data files were uploaded to [NEEShub \(2012a\)](#). No converted eccentric mass shaker data files were created.

CORRECTED DATA FILES

The GVDA data was further processed into corrected data. The procedure used to obtain the corrected structural response data was similar for all trials. The time signature of all subevent data files were converted from Unix time to relative time, in seconds, from the beginning of the subevent.

Corrected Structural Response Data Files

The corrected structural response data (accelerations and displacements) were created by applying mean removal to the converted data.

Corrected Eccentric Mass Shaker Data Files

The eccentric mass shaker data files were separated into subevents and acceleration signals were converted to engineering units and baseline corrected. The conversion of the accelerations to gravity (g) units is the same as for the structural response data. The pulse data marks in time the beginning of the sine wave, and no conversion was required. The converted data fields are similar to the unprocessed data, shown in Tables A1–A3.

Synchronized Structural Response and Eccentric Mass Shaker Data Files

During forced vibration testing using the eccentric mass shaker, EMS data including shaker pulse and structural accelerations were recorded on a distinct data acquisition system with no GPS time stamp and a higher frequency-sampling rate than the primary system (Q330 wireless data loggers). The higher sampling rate is necessary to evaluate phasing of the shaker force with adequate precision. It is necessary to synchronize and merge the EMS data with the SR data. In order to synchronize the data, the accelerometer records in the direction of shaking from the eccentric mass shaker data were decimated and then cross-correlated to channels 16 or 15 (depending on the direction of shaking) of the structural response data. We identified the time delay Δt between acceleration time series from the eccentric mass shaker and structural response data files by maximizing cross-correlation. This process is illustrated in Figure 9.

The synchronized eccentric mass shaker data was then used to compute shaker force histories using Equation 3. The EMS Pulse channel records a number of pulses per revolution of the eccentric mass. This pulse is recorded when the weight is aligned in the direction of loading, indicating that the angular position of the rotating mass, α is 0. Angle α at any other time can be evaluated through interpolation. The angular frequency of the rotating mass, ω , is evaluated at a given time directly from the number of pulses per unit time. With α and ω known, the shaker force due to rotation of the eccentric mass (first part of Equation 3) can be evaluated. This process is illustrated in Figure 10. The shaker force due to translation of the shaker mass center can be evaluated through the structural response data roof accelerometer. This component of the shaker force was excluded from the shaker force data files saved on NEEShub (2012a).

The corrected synchronized data files are organized in the same way as the corrected structural response data files, with additional data columns for the shaker angular frequency, shaker force, angular position of the shaker's rotating mass, and the eccentric mass shaker data accelerometer that was used for cross-correlation.

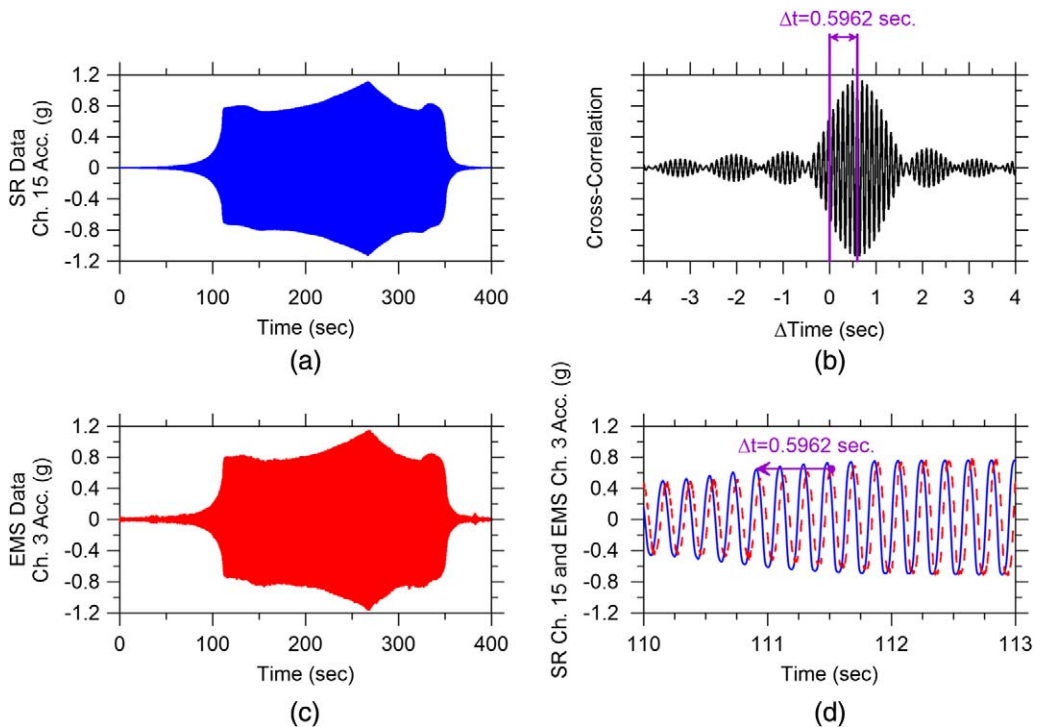


Figure 9. (a) Acceleration time series on test structure recorded by the structural response (SR) data acquisition system (Q330s); (b) adjacent and parallel acceleration time series recorded by the eccentric mass shaker (EMS) data acquisition system; (c) cross-correlation to identify time lag Δt between the two acceleration recordings; and (d) non-lag-corrected responses within a 3-second window with Δt labeled to indicate the lag required to match the two signals.

DATA USE

EXAMPLE APPLICATIONS

Data sets were developed to enable evaluation of foundation-soil interaction under field conditions for a wide range of frequencies and loading levels and also for variable conditions in the test specimens including: (1) relatively stiff and flexible super-structure (achieved with removable bracing); (2) variable base flexibility (data from different test locations); and (3) variable levels of relative moment-to-shear demands (shaking applied in long versus short direction of the oblong structure). Each of these conditions was varied because of their anticipated effect on the significance of SSI in the system response. For example, the structure-to-soil stiffness ratio ($h/(V_s T)$) (where h is the height for a single degree-of-freedom superstructure, V_s is the equivalent half-space shear wave velocity, and T is the fixed-base structure period) is an indicator of when inertial SSI effects are likely to be significant (typically for $h/(V_s T) > 0.1$; NIST 2012). This ratio varies from 0.17 to 0.45 for the various tests at the GDVA and WLA sites (Givens 2013). The ratios of structure

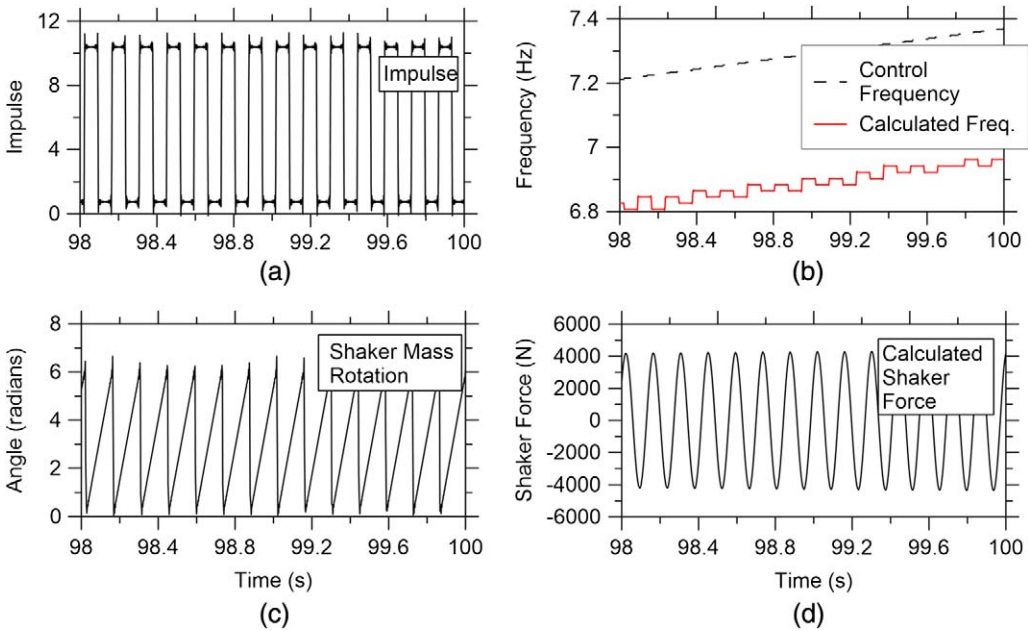


Figure 10. (a) Eccentric mass shaker pulse data; (b) interpolated angular position of the mass (α); (c) frequency of shaker mass rotation (as specified by control system and as calculated from pulse data); and (d) calculated eccentric mass shaker force.

height to foundation half-width, which control the relative moment-to-shear demands, measured in the two directions of shaking (h/B) are 1.4 and 2.8.

One application of the data is to apply system identification procedures with appropriate recorded input-output signals to establish fixed-base and flexible-base modal periods and damping ratios (e.g., [Stewart and Fenves 1998](#)). Data of this sort is useful for validating models for period lengthening (i.e., ratio of flexible- to fixed-base first-mode period) and foundation damping used in seismic design codes and other applications (e.g., [NIST 2012](#)). These system identification procedures can operate in either the time or frequency domains. Time domain procedures track the time variation of modal parameters, which is useful for identifying nonlinear responses. Frequency domain procedures provide time invariant properties for the duration of the signals that are used.

Another major application will involve inference from the data of foundation stiffness and damping in the form of impedance functions, which are widely used in sub-structure methods for seismic analysis of soil-foundation-structure systems (e.g., [NIST 2012](#)). For a two-dimensional problem, involving applied shear and moment loading to a foundation in a single horizontal direction (representing the condition in our tests for a given direction of shaking), the impedance function is a matrix that relates the foundation load vector $[V M]^T$ to the response vector $[u_f \theta_f]^T$ as follows ([Luco and Westmann 1971](#), [Veletsos and Wei 1971](#)):

$$\begin{bmatrix} \bar{k}_x & \bar{k}_{xy} \\ \bar{k}_{yx} & \bar{k}_{yy} \end{bmatrix} \begin{bmatrix} u_f \\ \theta_f \end{bmatrix} = \begin{bmatrix} V \\ M \end{bmatrix} \quad (4)$$

where V and M are base shear and moment, respectively; u_f and θ_f are foundation horizontal translation and rotation; and the \bar{k} terms are elements of the impedance matrix (the overbar indicates these elements are complex valued). For a surface foundation, the off-diagonal terms of the impedance matrix in Equation 4, \bar{k}_{xy} and \bar{k}_{yx} , should be zero, which allows the real part of \bar{k}_x to be understood (on a conceptual level) as the horizontal foundation stiffness (ratio of V to u_f) and the real part of \bar{k}_{yy} to be understood as the rotational foundation stiffness (ratio of M to θ_f). Damping of the foundation-soil system for a given vibration mode is related to the phase delay between the demand (e.g., base shear) and response (e.g., foundation displacement). This phase delay can be evaluated from the complex-valued impedance as:

$$\phi_j = \arctan\left(\frac{\text{imag}(\bar{k}_j)}{\text{real}(\bar{k}_j)}\right) \quad (5)$$

where j is a generic indicator of vibration mode.

Foundation impedance functions are known to be frequency dependant (Luco and Westmann 1971, Veletsos and Wei 1971). Frequency is typically expressed in dimensionless form for SSI applications as $a_0 = \omega B/V_s$, where B is the foundation half-width. Values of a_0 during testing at the WLA and GVDA sites ranged from 0.05 to 5.5. Impedance is also dependent on loading amplitude, because increasing shear strains in soil materials produce shear modulus reductions and soil damping increases. While the available instrumentation does not allow for direct measurements of shear strain, an approximate index of strain can be taken as the ratio of peak horizontal velocity of the foundation to soil V_s (used previously for free-field strains by Trifunac and Lee 1996, Paolucci and Smerzini 2008, and Brandenberg et al. 2009):

$$\gamma^i = \frac{\dot{u}_f}{V_s} \quad (6)$$

Superscript i indicates that γ^i is an index of shear strain (not a true strain). Values of this strain index ranged from well below the threshold for nonlinear soil behavior ($< \sim 10^{-4}\%$) to a maximum of approximately $2 \times 10^{-2}\%$ (Givens 2013 and Star 2011), for which soil non-linearity was pronounced as evidenced by reductions in foundation stiffness.

The inference of impedance functions from forced vibration data is non-trivial, but fundamentally can be achieved by inverting Equation 4 given known values of the demand and response vectors. Coupling terms can be evaluated from the inversion when forced vibration loading is applied at more than one degree of freedom (e.g., roof and foundation; de Barros and Luco 1995). Inversions of foundation impedance are typically carried out in the frequency-domain and have been applied in past work for low-strain (assumed elastic) conditions (e.g., Lin and Jennings 1984, Wong et al. 1988, Crouse et al. 1990, Tileylioglu et al. 2011). Details regarding the necessary calculations are beyond the scope of this article, but they are given in de Barros and Luco (1995) and Tileylioglu et al. (2011).

Once impedance functions are developed from forced vibration test data, it is of interest to compare them to predictions of theoretical models, which typically apply for idealized conditions such as rigid foundations and a uniform soil half-space. The results can be useful for the development of procedures for selecting representative half-space velocities given depth-variable velocities in the field. Deviations between theoretical and experimental results are also of interest, as they provide insights into the mechanics of the interaction problem not

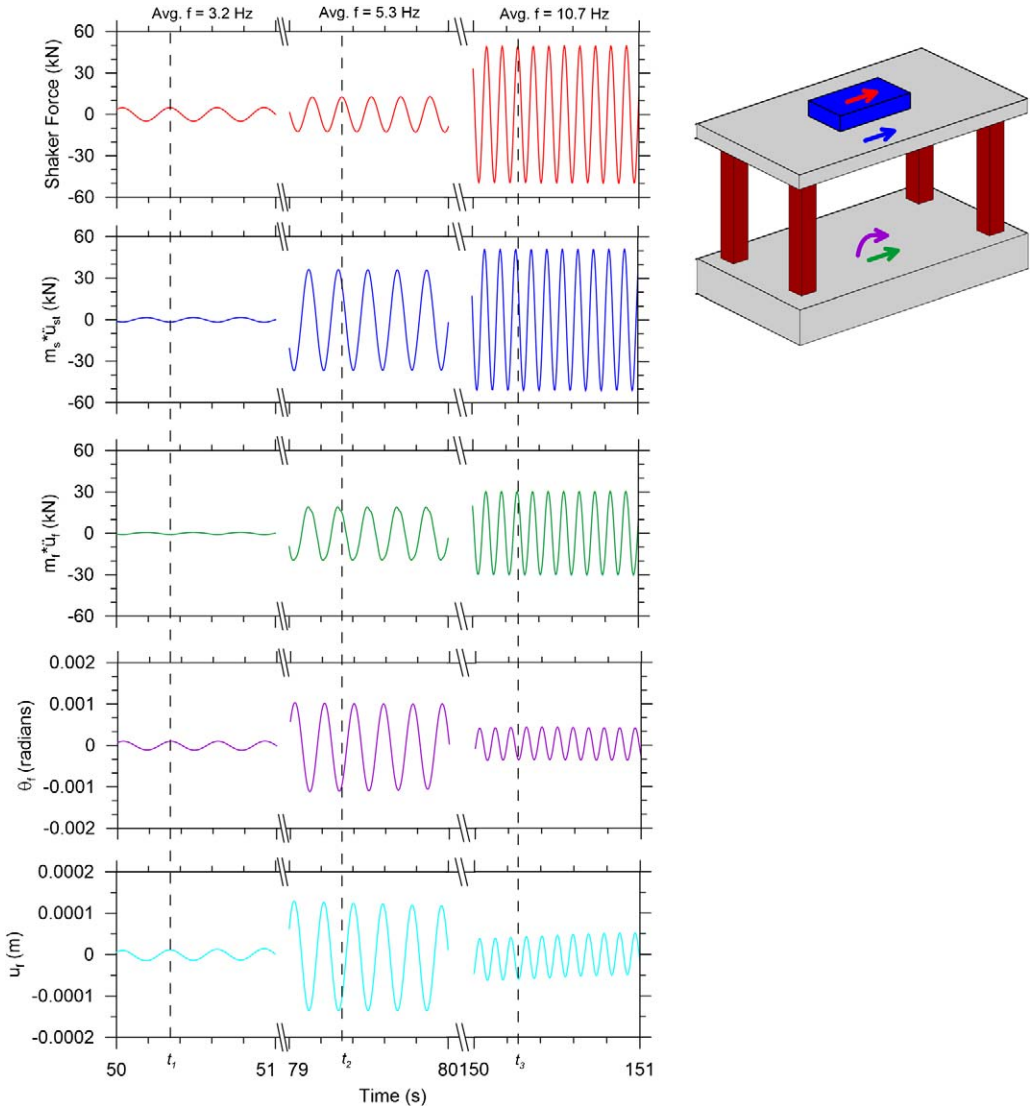


Figure 11. SSI test structure with shaker force, total inertia of top slab, inertia of base slab, rotation of base slab, and translational displacement of base slab.

revealed by simplified models. As an example, [Tileylioglu et al. \(2011\)](#) provide examples of how observed translational and rotational damping of a shallow foundation differs from theoretical models, and postulates that the differences may be caused by soil heterogeneity.

FEATURES OF THE DATA SET

Figure 11 illustrates some force-response features of the data set for an example of low amplitude shaking, where elastic soil behavior is expected. The figure shows time series of horizontal force demands (top three frames) and horizontal foundation rotations and displacements (bottom two frames) for a forced vibration-loading event. Three time intervals are shown—at a low frequency (*average freq.* = 3.2 Hz), near the resonant frequency of the SSI system (*average freq.* = 5.3 Hz), and at a high frequency (*average freq.* = 10.7 Hz). The horizontal inertial forces that are shown are (from top to bottom): shaker force, total inertia of top slab (taken as the product of the mass of top slab, including shaker frame, and horizontal acceleration $m_s \ddot{u}_{st}$), and total inertia of base slab (product of base slab mass and acceleration, $m_f \ddot{u}_f$). The foundation undergoes cyclic rotation and displacement as a result of the moment and base shear applied by force demands; time series of these responses are shown in the bottom frames (u_f, θ_f).

Information pertaining to the foundation damping can be gleaned from Figure 11, which shows that at time t_1 , with low frequency loading (below resonance), the shaker dominates the force demand, and its force history is nearly in-phase with the displacement and rotation. This is expected for a system with low levels of damping. At times t_2 , and t_3 , with higher frequency loading (at and above resonance), the top slab inertia dominates the force demand and is out of phase with the displacement and rotation, indicating much larger foundation damping than at low frequencies.

SUMMARY

Field-testing to measure soil-structure interaction (SSI) effects is useful to evaluate the applicability of analytical models for realistic field conditions and to guide the selection of model parameters. A test program was designed to provide high quality data for validation of SSI models under realistic boundary conditions, a wide range of load amplitudes, and a wide frequency range. Forced vibration tests were performed on a portable steel column structure. The test structure was reconfigurable to provide alternate structural stiffnesses and tests were performed with shaking applied in both the short and long directions of the oblong structure. The tests were performed at three test sites with different soil conditions including: the UCLA Structures Laboratory (nearly fixed-base conditions), the Wildlife Liquefaction Array (very soft clays and silts), and the Garner Valley Downhole Array (medium dense sands). The Garner Valley Downhole Array has an additional permanently installed structure that was also instrumented. Forced vibration-loading was provided by two different shakers installed on the structure and by a shaker truck. In addition, earthquake-loading events were recorded. Acceleration, displacement, and foundation pressure data was recorded and archived at the Network for Earthquake Engineering Simulations Research (NEESR) website, NEEShub, as project NEES-2008-0637.

ACKNOWLEDGMENTS

Support for this work was provided by the National Science Foundation (NSF). This work was completed as part of a multi-institutional NSF grand challenge (NSF 06-504 Program) project, “Mitigation of Collapse Risk in Vulnerable Concrete Buildings,” under Grant Number CMMI-0618804, and was documented in the Network for Earthquake Engineering Simulations Research (NEESR) website, NEEShub, as project NEES-2008-0637. Support by NEES@UCSB and NEES@UCLA was provided by the George E. Brown, Jr., Network for Earthquake Engineering Simulation (NEES) Program of the National Science Foundation (NSF) under Award Number CMMI-0927178.

This research made use of the field equipment, instrumentation, and technical expertise of NEES@UCLA and NEES@UCSB staff, including Ben Ferraro, Steve Keowen, Steve Kang, Dr. Alberto Salamanca, and Dr. Jamison Steidl. The NEES@UCSB also provided additional data from the permanently installed instrumentation. The NEES@UTexas team provided the use of their field equipment and performed additional geophysical testing at the field site. We thank the two anonymous reviewers for their valuable input on our paper.

APPENDIX

Additional information about sensors and experimental logs are available in the electronic supplement to the online version of this paper.

REFERENCES

- Brandenberg, S. J., Coe, J., Nigbor, R. L., and Tanksley, K., 2009. Different approaches for measuring ground strains during piledriving at a buried archeological site, *J. Geotech. & Geoenviron. Eng.* **135**, 1101–1112.
- Crouse, C. B., Hushmand, B., Luco, J. E., and Wong, H. L., 1990. Foundation impedance functions: Theory versus experiment, *J. Geotech. Eng.* **116**, 432–449.
- de Barros, F. C. P., and Luco, J. E., 1995. Identification of foundation impedance functions and soil properties from vibration tests of the Hualien containment model, *Soil Dyn. & Eqk. Eng.* **14**, 229–248.
- Fadum, R. E., 1948. Influence values for estimating stresses in elastic foundations, *Proc. 2nd Int. Conf. Soil Mechs. and Foundn. Eng.*, Rotterdam, vol. **3**, 77–84.
- Givens, M. J., 2013. Dynamic Soil-Structure Interaction of Instrumented Buildings and Test Structures, Ph.D. Thesis, University of California, Los Angeles.
- Kinematics, Inc., 2005. *EpiSensor, Force Balance Accelerometer, Model FBA ES-T*, Pasadena, CA.
- Lin, A. N., and Jennings, P. C., 1984. Effect of embedment on foundation-soil impedances, *J. Eng. Mech.* **110**, 1060–1075.
- Luco, J. E., and Wong, H. L., 1990. Forced vibration of the Lotung containment model: Theory and observations, *J. Eng. Mech.* **116**, 845–861.
- Luco, J. E., and Westmann, R. A., 1971. Dynamic response of circular footings, *J. of the Eng. Mech. Div.* **97**, 1381–1395.
- Network for Earthquake Engineering Simulations (NEEShub), 2012a. Mitigation of Collapse Risk in Vulnerable Concrete Buildings, Project NEES-2008-0637, available at <https://nees.org/warehouse/project/637>.

- Network for Earthquake Engineering Simulations (NEEShub), 2012b. Permanently Instrumented Field Sites, Project NEES-2007-0353, available at <https://nees.org/warehouse/experiments/353>.
- Network for Earthquake Engineering Simulations at University of California, Los Angeles (NEES@UCLA), 2012. Equipment, available at <http://nees.ucla.edu/equipment.html>.
- Network for Earthquake Engineering Simulations at University of California, Santa Barbara (NEES@UCSB), 2012. Wildlife Liquefaction Array and Garner Valley Downhole Array, available at <http://nees.ucsb.edu/facilities/wla> and <http://nees.ucsb.edu/facilities/gvda>.
- Network for Earthquake Engineering Simulations at University of Texas, Austin (NEES@UTexas), 2012. Available at <http://nees.utexas.edu/Equipment.shtml>.
- National Institute of Standards and Technology (NIST), 2012. *Soil-structure Interaction for Building Structures, Report No. NIST GCR 12-917-21*, U.S. Department of Commerce, Washington, D.C.
- Paolucci, R., and Smerzini, C., 2008. Earthquake-induced transient ground strains from dense seismic networks, *Earthquake Spectra* **24**, 453–470.
- Reinert, E. T., Brandenberg, S. J., Stewart, J. P., and Moss, R. E. S., 2012. Dynamic field test of a model levee founded on peaty organic soil using an eccentric mass shaker, *15th World Conf. on E.Q. Eng.*, Lisbon, Portugal.
- Star, L. M., 2011. Seismic Vulnerability of Structures: Demand Characteristics and Field Testing to Evaluated Soil-Structure Interaction Effects, Ph.D. Thesis, University of California, Los Angeles.
- Steidl, J. H., Youd, T. L., and Nigbor, R. L., 2004. Research opportunities at the NEES permanently instrumented field sites, *13th World Conf. on E.Q. Eng. Vancouver B.C., Canada*, 1–6 August 2004, Vancouver, BC, Canada.
- Steller, R., 1996. *New Borehole Geophysical Results at GVDA*, available at <http://nees.ucsb.edu/facilities/gvda>.
- Stewart, J. P., and Fenves, G. L., 1998. System identification for evaluating soil-structure interaction effects in buildings from strong motion recordings, *Earthquake Engng. & Struct. Dyn.* **27**, 869–885.
- Stewart, J. P., Fenves, G. L., and Seed, R. B., 1999. Seismic soil-structure interaction in buildings II: Empirical findings, *J. Geotech. & Geoenv. Eng.* **125**, 38–48.
- Stokoe, K. H., Kurtulus, A., and Menq, F., 2004. *Data Report Measurements at the NEES Garner Valley Test Site, California*, University of Texas, Austin.
- Stokoe, K. H., Lin, Y., Menq, F., and Cox, B. R., 2010. *Wildlife Refuge Liquefaction Field Site Shear Wave Velocity Measurements using Spectral-Analysis of Surface Waves (SASW) Test*, NEES@UTexas Equipment Site, Austin, TX.
- Tang, H. T., Tang, Y. K., and Stepp, J. C., 1990. Lotung large-scale seismic experiment and soil-structure interaction method validation, *Nucl. Eng. & Des.* **123**, 397–412.
- Tileyioglu, S., Stewart, J. P., and Nigbor, R. L., 2011. Dynamic stiffness and damping of shallow foundation from forced vibration of a field test structure, *J. Geotech. & Geoenv. Eng.* **137**, 344–353.
- Trifunac, M. D., and Lee, V. W., 1996. Peak surface strains during strong earthquake motion, *Soil Dyn. & Eqk. Eng.* **15**, 311–319.
- Veletsos, A. S., and Wei, Y. T., 1971. Lateral and rocking vibrations of footings, *J. of Soil Mech. & Foundns. Div.* **97**, 1227–1248.

- Wong, H. L., and Luco, J. E., 1990. Seismic response of the Lotung containment model: Theory and observations, *J. of Soil Mech. & Foundns. Div.* **116**, 1332–1350.
- Wong, H. L., Trifunac, M. D., and Luco, J. E., 1988. A comparison of soil-structure interaction calculations with results of full-scale forced vibration tests, *Soil Dyn. & Eqk. Eng.* **7**, 22–31.
- Yamada, S., Hyodo, M., Orense, R. P., Dinesh, S. V., and Hyodo, T., 2008. Strain-dependent dynamic properties of remolded sand-clay mixtures, *J. of Geotech. & Geoenv. Eng.* **134**, 972–981.
- Youd, T. L., and Holzer, T. L., 1994. Piezometer performance at wildlife liquefaction site, California, *J. of Geotech. Eng.* **120**, 975–995.
- Youd, T. L., Steidl, J. H., and Nigbor, R. L., 2004a. Lessons learned and need for instrumented liquefaction sites, *Soil Dyn. & Eqk. Eng.* **24**, 639–646.
- Youd, T. L., Bartholomew, H. A. J., and Proctor, J. S., 2004b. *Geotechnical Logs and Data From Permanently Instrumented Sites: Garner Valley Downhole Array (GVDA) and Wildlife Liquefaction Array (WLA)*, University of California, Santa Barbara.

(Received 15 May 2014; accepted 18 April 2015)